

Carl J. Schreck III<sup>1</sup>, Lei Shi<sup>2</sup>, and James P. Kossin<sup>2</sup><sup>1</sup>Cooperative Institute for Climate and Satellites-NC (CICS-NC), Asheville, NC<sup>2</sup>NOAA's National Climatic Data Center (NCDC), Asheville, NC

## 1. INTRODUCTION

The Madden–Julian Oscillation (MJO; Madden and Julian 1994; Zhang 2005) and equatorial waves (Kiladis et al. 2009) have frequently been identified using proxies for convection such as outgoing longwave radiation (OLR). These data are suitable for the Eastern Hemisphere where deep tropical convection is commonplace. However, the convection becomes weaker in the Western Hemisphere, even as the wave signals persist in the upper troposphere. Inter-satellite calibration techniques have recently produced a homogeneous 32-year dataset of upper tropospheric water vapor (UTWV). These data will be used to revisit the climatologies of the MJO and equatorial waves.

## 2. DATA AND METHODS

Daily Interpolated OLR data are obtained from NOAA/OAR/ESRL/PSD. These data are observed with the Advanced Very High Resolution Radiometer (AVHRR) sensor on the NOAA polar orbiting satellites. They were binned into daily 2.5° latitude–longitude grids and missing values were filled following Liebmann and Smith (1996). For any given day, only one satellite was used, generally the one with the 1430 equatorial crossing time. Because of OLR's strong diurnal cycle, day and night passes were binned and interpolated separately. The resulting grids were then averaged together to produce the daily values.

The UTWV data are channel 12 brightness temperatures from the High Resolution Infrared Sounder (HIRS) sensor on the NOAA and the European MetOp polar-orbiting satellites. As part of NOAA's Climate Data Record (CDR) program, the data were calibrated for inter-satellite differences following Shi and Bates (2011). This calibration allows us to use data from all satellites, regardless of equatorial crossing time, for maximum coverage. The

calibrated data were binned into daily 2.5° grids to match the OLR. Missing values were interpolated using a similar scheme as the OLR (Liebmann and Smith 1996). Notably, the daytime and nighttime passes were not treated separately for UTWV because of its smaller diurnal cycle (Lindfors et al. 2011).

The fraction of variance associated with the MJO and each equatorial wave type was calculated as follows. First, the 32-year mean and the first three harmonics of the seasonal cycle were subtracted from the original data. Second, these daily anomalies were divided by each grid point's standard deviation. The resulting standardized anomalies were then filtered for the wavenumbers and frequencies associated with each wave type. The mean of the square of these filtered values represents the fraction of the total variance that is associated with each wave type.

## 3. RESULTS

Figure 1 shows the zonal wavenumber–frequency spectra for UTWV following the methodology of Wheeler and Kiladis (1999). This figure is comparable to their Fig. 6, which showed the same spectra for OLR. As with OLR, many of the UTWV signals fall between the dispersion curves for shallow water equatorial waves with equivalent depths between 8 m and 90 m (black lines). The UTWV signals are particularly strong for Kelvin waves and equatorial Rossby (ER) waves, both of which are symmetric about the equator. Meanwhile, the anti-symmetric signals such as  $n = 0$  mixed Rossby–gravity (MRG) and eastward inertio-gravity (EIG) waves are weaker in the UTWV data.

Tropical depression (TD)-type disturbances, often termed “easterly waves”, are not associated with any shallow water solution, but their signals appear as westward propagation with periods of 2–10 days (Fig. 1). The TD signals are stronger in UTWV than in OLR (not shown). The MJO is another signal that is not associated with any shallow water dispersion curve but shows prominently in both the symmetric and anti-symmetric spectra. The blue

---

\* Corresponding author address: Carl J. Schreck III, Cooperative Institute for Climate and Satellites-NC (CICS-NC), 151 Patton Ave, Asheville, NC 28801; e-mail: carl@cicsnc.org

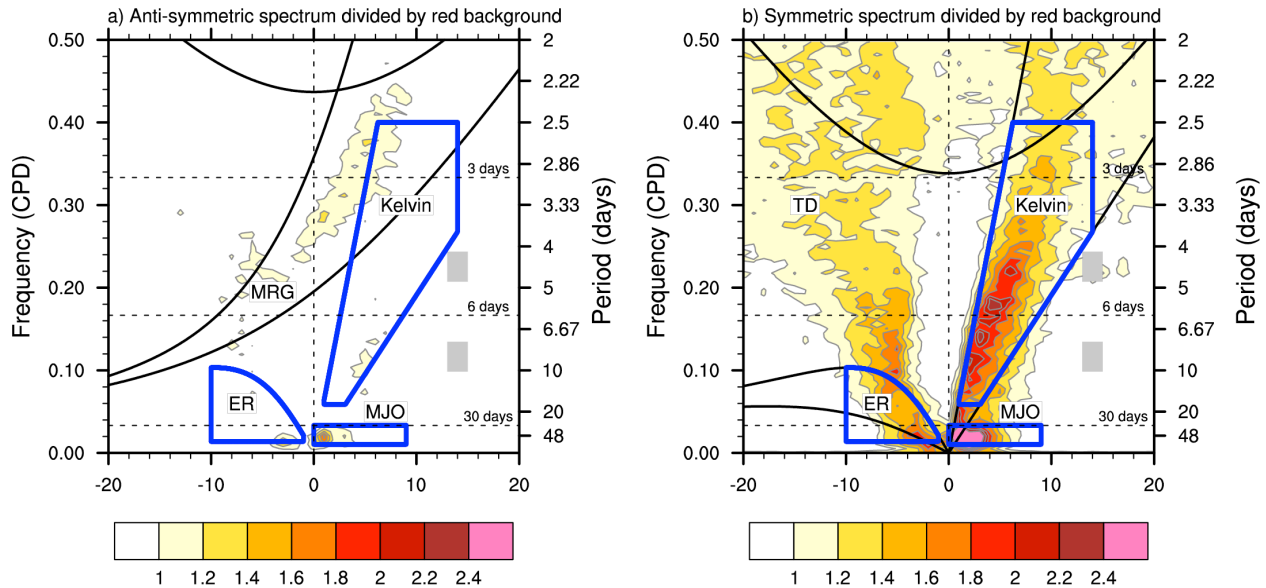


Figure 1. Wavenumber–frequency spectra of UTWV from 15°S–15°N divided a red background. Signals are anti-symmetric about the equator in (a) and symmetric in (b). Black lines denote shallow water equatorial wave dispersion curves for equivalent depths of 8 m and 90 m. Blue boxes define the filter bands used in this study.

boxes in Fig. 1 identify filter bands that will be used to identify signals associated with the MJO, ER waves, and Kelvin waves. These filters are adapted from Kiladis and coauthors (Wheeler and Kiladis 1999; Straub and Kiladis 2002; Kiladis et al. 2005, 2009), who used them to identify prominent modes of variability in OLR.

Figure 2 shows the fraction of the total OLR and UTWV variance that falls within the MJO filter band during December–May (DJFMAM) and June–November (JJASON). Consistent with previous studies of the MJO (Zhang and Dong 2004; Roundy and Frank 2004), its DJFMAM OLR signal (Fig. 2a) is concentrated in the

equatorial Indian Ocean and the northern coast of Australia. These signals also appear in UTWV (Fig. 2b) along with some notable differences. In general, the fraction of variance associated with the MJO is larger in UTWV compared with OLR. The MJO also accounts for more than 12% of the variance over a band that nearly encircles the globe around 20°N. This signal is absent in OLR.

The MJO signals are weaker during JJASON (Figs. 2c,d). The OLR signals are still concentrated on the Indian Ocean. A secondary signal also appears over the eastern North Pacific. This eastern Pacific signal plays an

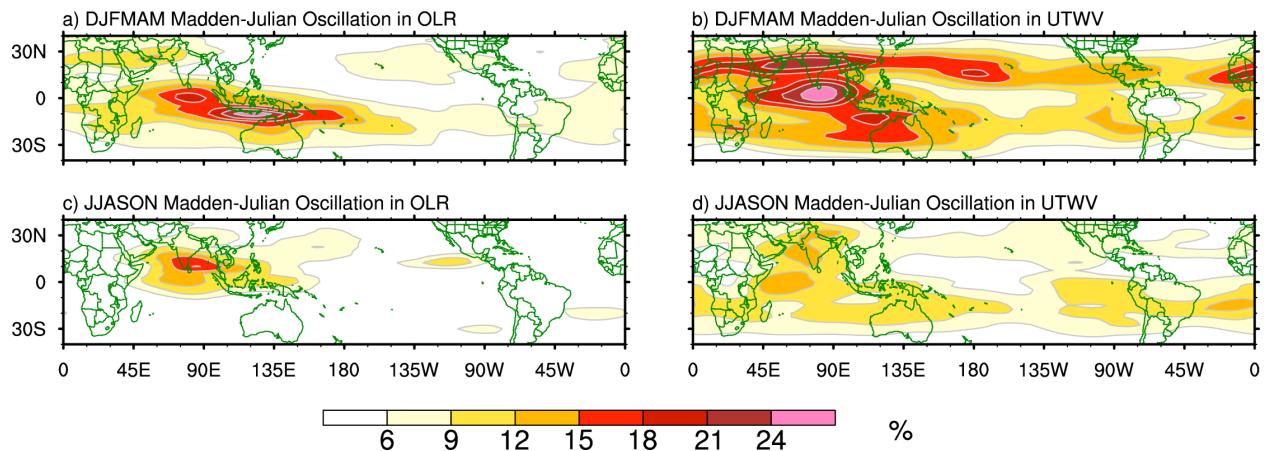


Figure 2. Percentage of the total OLR (left) and UTWV (right) variance during December–May (top) and June–November (bottom) that falls within the MJO filter band.

important role in modulating tropical cyclone activity in that region and over the Gulf of Mexico (Molinari et al. 1997; Maloney and Hartmann 2000a; b; Aiyyer and Molinari 2008). The UTWV signals are more diffuse, and the eastern North Pacific signal is lacking. Interestingly, the MJO band accounts for at least 9% of the UTWV variance over broad portions of the subtropical Southern Hemisphere. These signals may be associated with tropical–extratropical interactions.

#### 4. CONCLUSIONS

This study illustrates the utility of UTWV for investigating and monitoring the MJO and equatorial waves. As with OLR, the MJO and equatorial wave signals stand out above the red background in UTWV (Fig. 1). The MJO actually accounts for a larger fraction of variance in UTWV than in OLR (Fig. 2). The UTWV signals are also more zonally uniform and contain considerable subtropical variance. These subtropical signals are likely to be associated with compensating vertical motion associated with the equatorial convection. They may also be associated with tropical–extratropical interactions. Monitoring tropical variability in UTWV and OLR together may lead to improved intraseasonal forecasts. To that end, these data are currently being analyzed in near-real time at: <http://monitor.cicsnc.org/mjo/>.

#### REFERENCES

- Aiyyer, A., and J. Molinari, 2008: MJO and tropical cyclogenesis in the Gulf of Mexico and eastern Pacific: Case study and idealized numerical modeling. *J. Atmos. Sci.*, **65**, 2691-2704.
- Kiladis, G. N., K. H. Straub, and P. T. Haertel, 2005: Zonal and vertical structure of the Madden–Julian oscillation. *J. Atmos. Sci.*, **62**, 2790-2809.
- Kiladis, G. N., M. C. Wheeler, P. T. Haertel, K. H. Straub, and P. E. Roundy, 2009: Convectively coupled equatorial waves. *Rev. Geophys.*, **47**, RG2003, doi:10.1029/2008RG000266.
- Liebmann, B., and C. A. Smith, 1996: Description of a complete (interpolated) outgoing longwave radiation dataset. *Bull. Amer. Meteor. Soc.*, **77**, 1275–1277.
- Lindfors, A. V., I. A. Mackenzie, S. F. B. Tett, and L. Shi, 2011: Climatological Diurnal Cycles in Clear-Sky Brightness Temperatures from the High-Resolution Infrared Radiation Sounder (HIRS). *Journal of Atmospheric and Oceanic Technology*, **28**, 1199-1205.
- Madden, R. A., and P. R. Julian, 1994: Observations of the 40–50-Day Tropical Oscillation—A Review. *Mon. Wea. Rev.*, **122**, 814-837.
- Maloney, E. D., and D. L. Hartmann, 2000a: Modulation of hurricane activity in the Gulf of Mexico by the Madden-Julian oscillation. *Science*, **287**, 2002-2004.
- Maloney, E. D., and D. L. Hartmann, 2000b: Modulation of eastern North Pacific hurricanes by the Madden–Julian oscillation. *J. Climate*, **13**, 1451-1460.
- Molinari, J., D. Knight, M. Dickinson, D. Vollaro, and S. Skubis, 1997: Potential vorticity, easterly waves, and eastern Pacific tropical cyclogenesis. *Mon. Wea. Rev.*, **125**, 2699-2708.
- Roundy, P. E., and W. M. Frank, 2004: A climatology of waves in the equatorial region. *J. Atmos. Sci.*, **61**, 2105-2132.
- Shi, L., and J. J. Bates, 2011: Three decades of intersatellite-calibrated High-Resolution Infrared Radiation Sounder upper tropospheric water vapor. *J. Geophys. Res.*, **116**, 13 PP.
- Straub, K. H., and G. N. Kiladis, 2002: Observations of a convectively coupled Kelvin wave in the eastern Pacific ITCZ. *J. Atmos. Sci.*, **59**, 30-53.
- Wheeler, M., and G. N. Kiladis, 1999: Convectively coupled equatorial waves: Analysis of clouds and temperature in the wavenumber–frequency domain. *J. Atmos. Sci.*, **56**, 374-399.
- Zhang, C., 2005: Madden-Julian oscillation. *Rev. Geophys.*, **43**, RG2003, doi:10.1029/2004RG000158.
- Zhang, C., and M. Dong, 2004: Seasonality in the Madden–Julian Oscillation. *J. Climate*, **17**, 3169-3180.